Adsorption and Diffusion of *n*-Hexane/2-Methylpentane Mixtures in Zeolite Silicalite: Experiments and Modeling

D. Schuring,*,† A. O. Koriabkina,† A. M. de Jong,‡ B. Smit,§ and R. A. van Santen†

Laboratory of Inorganic Chemistry and Catalysis and Accelerator Laboratory, Schuit Institute of Catalysis, Eindhoven University of Technology, P.O. Box 513, 5600 MB Eindhoven, The Netherlands, and Department of Chemical Engineering, University of Amsterdam, Nieuwe Achtergracht 166, 1018 WV Amsterdam, The Netherlands

With the tracer-exchange positron emission profiling (TEX-PEP) technique, the reexchange process of radioactively labeled molecules with a steady-state feed stream can be measured inside a zeolite-packed bed reactor. When the experimental tracer-exchange curves are modeled, values for the micropore diffusion and adsorption constant can be obtained. As one can choose which component to label, this technique is ideally suited for studying multicomponent diffusion. In the present study, this technique has been used to measure the diffusive and adsorptive properties of an *n*-hexane/2-methylpentane mixture in zeolite silicalite. The measurements were performed at different ratios of *n*-hexane and 2-methylpentane in the gas phase at a constant total hydrocarbon pressure of 6.6 kPa and a temperature of 433 K. A slight preference for the adsorption of *n*-hexane was found because it is entropically more favorable to adsorb these molecules as they have no preferential siting in the zeolite pores. The diffusivity of the slowly moving 2-methylpentane is not strongly affected by the presence of the fast moving *n*-hexane. The mobility of the linear alkane however strongly decreases with increasing 2-methylpentane ratio and suddenly drops at a loading of approximately three 2-methylpentane molecules per unit cell. This is caused by the fact that the branched alkanes are preferentially sited in the intersections between the straight and zigzag channels of silicalite and therefore effectively block the zeolite pore network. These results show that the adsorptive properties of the components and the structure of the zeolite network play an important role in the behavior of multicomponent mixtures in zeolites.

I. Introduction

Diffusion and adsorption of hydrocarbons in zeolites have received a lot of attention in the last few decades.[1,2] This is due in no small part to the vast number of applications of these materials in the petrochemical industry, e.g., as catalysts in cracking and hydroisomerization processes and as molecular sieves in separation processes. For all these applications, a thorough understanding of the diffusive and adsorptive properties of molecules inside these materials is of vital importance as these greatly influence the performance of the catalytic or separation processes. When used as, for example, a catalyst or molecular sieve, at least two, or even more, species are present inside the zeolite. Surprisingly, most studies are focused on the diffusion and adsorption of single components only. In the first place, this results from the fact that most conventional methods for studying mass transfer in zeolites, like the gravimetric and volumetric methods, are intrinsically unable to distinguish between different types of molecules. Furthermore, it is generally assumed that diffusion in multicomponent systems can be predicted from single-component data.

Only in recent years, the number of investigations on multicomponent mixtures is increasing. However, most of these studies are concerned with small molecules only, like methane/

xenon,[3,4] ethane/ethene,[5] and *n*-butane/methane,[6] and the majority of these studies is focused on the sorption thermodynamics, often making use of molecular simulations. Most experimental data are obtained with techniques such as NMR and quasielastic neutron scattering and at relatively low temperatures. Among the few papers dealing with longer hydrocarbons are the work of Choudhary et al. (aromatics in ZSM-5)[7] and Niessen and Karge (xylene/benzene mixtures)[8] and work on cyclic, branched, and linear hydrocarbons in silicalite membranes by Funke and co-workers.[9] Recently, Masuda and co-workers[10] reported results on *n*-heptane/*n*-octane and *ortho*- and *meta*-xylene mixtures at elevated temperatures. They concluded that while the diffusivity of the slow component with increasing amounts of the fast components remains constant, the diffusivity of the fast component decreases monotonically with the increasing fraction of slow components. This is in line with results obtained for the mixtures of smaller components.

A relatively new technique capable of studying adsorption and diffusion of multicomponent mixtures is positron emission profiling (PEP), which makes use molecules labeled with a positron-emitting isotope. This technique is based on coincident detection of the γ-photons resulting from the annihilation of a positron emitted by the radioactive isotope with an electron from the chemical environment. Because the annihilation produces a pair of γ-photons traveling in (almost) opposite directions, the exact location of the decay event can be determined by coincident detection of these photons. Due to the high penetrating power of the γ-rays, a great advantage of this technique is
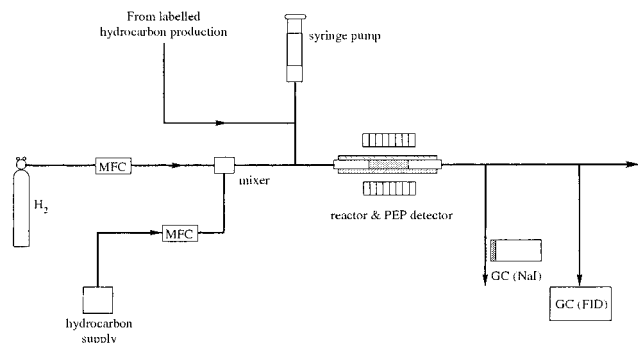
Figure 1. Schematic diagram of the reactor setup used for the tracer-exchange positron emission profiling measurements.

that in situ measurements can be performed on ordinary laboratory-scale reactors at normal reaction conditions. Furthermore, because labeled molecules are used, one has the possibility of only labeling one component in a mixture thus making it possible to study only this component. The positron emission profiling technique has been described in detail in Anderson et al.[11,12] and was already used successfully for studying single-component diffusion in biporous-packed beds of zeolites.[13] Recently, this technique has been extended to incorporate tracer-exchange experiments.[14] With these experiments, a continuous stream of labeled molecules is injected into a steady-state feed stream. The rate at which the exchange between labeled and nonlabeled molecules takes place is determined by the diffusion of the adsorbates inside the zeolite channels. Through the study of the exchange process, information can be obtained about diffusion and adsorption inside the zeolite crystals. The advantage of using tracer-exchange experiments over using transient experiments is that one is assured that the entire experiment is performed under steady-state conditions so that the true self-diffusion constant is measured.

In this paper, the tracer-exchange positron emission profiling (TEX-PEP) technique is being used to study the adsorption and diffusion of *n*-hexane/2-methylpentane mixtures in zeolite silicalite. These systems were chosen because of their practical applications, the availability of other (theoretical) studies, and the peculiar adsorption behavior observed for the single components.[15] With total pressure kept constant, the adsorptive and diffusive behaviors of *n*-hexane and 2-methylpentane have been studied as a function of the *n*-hexane/2-methylpentane ratio in the gas phase. The rest of this paper will deal with the experimental details, the model used for evaluating the experiments, and the results obtained.

II. Experimental Setup

For the experiments conducted in this study, the same setup was used as that described earlier in the work of Schumacher et al.[14] The positron-emitting ^{11}C isotope is produced by irradiation of a nitrogen target with 12 MeV protons from the 30 MeV AVF cyclotron at the Eindhoven University of Technology. The resulting ^{11}C is then transferred as CO/CO_2 to the setup for the production of labeled hydrocarbons. Details of the homologation process used for the production of labeled *n*-hexane and 2-methylpentane can be found in Cunningham et al.[16] After separation of the different products produced in this process, the desired labeled species is collected in a syringe.

Figure 1 shows a schematic diagram of the reactor system used in the TEX-PEP experiments. During the tracer-exchange experiments, a constant flow of nonlabeled hydrocarbons in a hydrogen carrier stream was fed into the reactor. The *n*-hexane/

2-methylpentane/hydrogen mixture was produced using a controlled evaporator and mixer (CEM) mixing unit consisting of two branches each of which was equipped with a mass flow controller (MFC). By the use of these controllers for the *n*-hexane and 2-methylpentane branch, the composition of the mixture can be set. The total flow rate of hydrocarbons and carrier gas was set to a value of 80.2 mL/min.

For a tracer-exchange experiment, a quantity of labeled molecules of either *n*-hexane or 2-methylpentane was produced and continuously injected into the feed stream using a syringe pump. The tracer-exchange and tracer-reexchange process could then be monitored using the PEP detector by either turning the tracer flow on or turning the tracer flow off. The PEP detector measures the concentration by reconstructing the position of the positron-emitting isotopes via coincident detection of the two *γ*-photons emitted in opposite directions during an annihilation event. With the current setup, the concentration of the labeled alkanes is then measured at 17 different positions along the reactor axis with a spatial resolution of 3.05 mm and a minimum sampling time of 0.5 s. A detailed description of the detection system can be found in Mangnus et al.[17] and Anderson et al.[11] Because of switching effects,[14] the reexchange process yields more reliable results, and only this stage of the experiments was used for determining the kinetic parameters.

For the experiments, a sample of silicalite-1 was obtained from the Shell Research and Technology Centre in Amsterdam. The zeolite crystals in this sample have a very regular shape with dimensions of 150 *μ*m × 50 *μ*m × 30 *μ*m. Because of the large size, it was not necessary to press these crystals into larger pellets. The large crystal size furthermore ensures that processes taking place inside the zeolite are really dominating the transport properties inside the bed. The bed porosity was determined from the pressure drop over the bed using the Ergun relation, yielding a value of $\epsilon = 0.44$. The length of the zeolite bed was 3 cm. Prior to being used in experiments, the zeolite sample was activated for at least 1 h at 673 K in a hydrogen stream. The *n*-hexane and 2-methylpentane gases used for the constant nonlabeled flow had a purity of at least 99.9%.

III. Modeling the Tracer-Exchange Process

For interpretation of the data from the TEX-PEP experiments, a mathematical model is needed for describing the reexchange process in the zeolite reactor bed. A common way to describe diffusion in packed beds is use of a system of diffusion equations describing the mass transport in the zeolite bed and inside the crystals.[1,18,19] The model used in this study basically is a modification of the equations used by Noordhoek et al.[20] It is assumed that the transport of molecules occurs via convection and axial diffusion in the space between the crystals, adsorption−desorption at the crystal surface, and diffusion inside the pores of the crystals. Furthermore, it is assumed that the crystals have a spherical shape. This approximation is commonly made in the literature and has been shown to be quite reasonable.[1] This is probably due to the random orientation of the crystals inside the reactor, which makes it difficult to really explicitly account for the particle shape. As only one component is detected during the experiments, single-component equations can be used to model its behavior. The parameters describing the different processes in the bed will then be effective values for the transport of this component in the mixture.

A. The Model Equations. Transport in the fluid phase inside the packed bed takes place through convection, axial diffusion, and flow to or from the zeolite crystals. A mass balance for a small volume element of the bed results in the following

equation for the concentration, C_z, in the gas phase:

$$\frac{\partial C_z}{\partial t} = D_{ax}\frac{\partial^2 C_z}{\partial z^2} - v_{int}\frac{\partial C_z}{\partial z} + \frac{3(1-\epsilon)}{\epsilon R_c}N_c \tag{1}$$

In this equation, z is the coordinate along the reactor axis, D_{ax} is the axial diffusion coefficient, and v_{int} is the interstitial velocity, which can be calculated from the gas flow speed v_{sup} using $v_{int} = v_{sup}/\epsilon$. The axial diffusivity can be calculated from the molecular diffusion coefficient of the component. For R_c, the radius of the crystals, the equivalent spherical particle radius, $\bar{R}_c$, is taken, defined as the radius of the sphere having the same external surface area to volume ratio.[1] For the crystal size used in this study, this yields a value of 25 μm.

The boundary conditions used for the bed equation are identical to the ones used in Noordhoek et al.[20] For the column entrance, a mass balance (and by neglecting the diffusional term just in front of the column) yields

$$\frac{\partial C_{z,0^+}}{\partial z} = \frac{v_{int}}{D_{ax}}(C_{z,0^+} - C_{z,0^-}) \tag{2}$$

in which $C_{z,0^-}$ and $C_{z,0^+}$ are the fluid phase concentrations just in front of and just after the column entrance, respectively. For TEX-PEP experiments, concentration just in front of the packed bed is given by the Heaviside step function

$$C_{z,0^-}(t) = C_0, \quad t \leq 0$$

$$C_{z,0^-}(t) = 0, \quad t > 0 \tag{3}$$

At the column exit, the diffusional term is neglected, turning eq 1 into a first-order equation which can be used as a boundary condition.

The term N_c equals the mass flux through the boundary of the zeolite and is determined by the rate-limiting step for adsorption−desorption at the crystal boundary. It is assumed that external mass transfer resistance due to the diffusion through the laminar fluid film surrounding the particles can be neglected as this process is much faster than diffusion inside the zeolite crystals. This has been confirmed by comparing simulations with and without this process included in the model, which shows that neglecting the external film mass transfer resistance does not influence the results.

The model of Nijhuis et al.[19] explicitly accounts for adsorption−desorption at the crystal boundary, assuming Langmuir adsorption kinetics. As the TEX-PEP experiments are conducted under steady-state conditions, this mechanism can be replaced by a simple first-order adsorption−desorption process

$$N_c = k_d C_x(R_c,z,t) - k_a C_z(z,t) \tag{4}$$

in which k_a and k_d are the adsorption and desorption constants in meters per second. This equation furthermore has the advantage that k_a and k_d have the same dimensions and that there is no need to determine the number of adsorption sites.

Transport inside the zeolite crystals occurs through diffusion inside the zeolite pores. Although it is known that diffusion in zeolites is generally anisotropic,[21] the random orientation of the crystals inside the reactor justifies the approximation that micropore diffusion can be described as an isotropic process. A mass balance for zeolite crystals yields for the adsorbed phase concentration, C_x, in the crystals

$$\frac{\partial C_x}{\partial t} = D_c\left(\frac{\partial^2 C_x}{\partial x^2} + \frac{2}{x}\frac{\partial C_x}{\partial x}\right) \tag{5}$$

in which D_c is the intracrystalline diffusivity and x is the radial coordinate of the crystal. In principle, the value of the diffusion constant depends on the concentration of both components. However, during the experiments, the total concentration does not change and D_c can thus be regarded as constant during a single measurement. The boundary condition at the center of the particle is obtained from symmetry reasons:

$$\left.\frac{\partial C_x}{\partial x}\right|_{x=0} = 0 \tag{6}$$

At the crystal boundary, the flow to the surface must be equal to the desorption rate at the crystal boundary at $x = R_c$:

$$\left.D_c\frac{\partial C_x}{\partial x}\right|_{x=R_c} = k_a C_z(z,t) - k_d C_x(R_c,z,t) \tag{7}$$

The initial conditions can be found by realizing that at the start of a tracer-reexchange process, the system is in equilibrium. Assuming that the injected tracer concentration initially is equal to C_0, the initial conditions are given by

$$C_z(z,t=0) = C_0$$

$$C_x(x,z,t=0) = K_a C_0 \tag{8}$$

in which K_a is the adsorption equilibrium constant given by $K_a = k_a/k_d$.

B. Solving the Model. The equations described above have been solved using the numerical method of lines.[22] This procedure has been described in detail in Noordhoek et al.[20] In short, this is done by discretizing the spatial coordinates (and spatial derivatives), converting the system of partial differential equations into a set of ordinary differential equations (ODEs). These ODEs can then be solved using an ordinary numerical integration routine. Solving the model yields values for the concentration at each bed and crystal grid point. Because the PEP detector measures the total concentration of labeled molecules in a certain section of the catalyst bed, volume averaging has to be applied to simulate the response of the PEP detector. The average microparticle concentration at position z inside the reactor bed equals

$$\langle C_x(z,t)\rangle = \frac{3}{R_c^3}\int_0^{R_c} C_x(x,z,t)x^2\,dx \tag{9}$$

Because the crystal concentration, C_x, is only known at the grid points, this integral has to be evaluated numerically. The total concentration at position z can than be calculated by averaging over the bed and crystal concentration as follows:

$$\langle C_{tot}(z,t)\rangle = \epsilon C_z(z,t) + (1-\epsilon)\langle C_x(z,t)\rangle \tag{10}$$

Estimation of the different parameters, i.e., the adsorption−desorption and diffusion in the zeolite crystals, is done by fitting the modeled concentration profiles to the measured ones using a least-squares Levenberg−Marquardt algorithm.[23] All the other parameters were determined experimentally.

C. Adsorption−Desorption at the Crystal Boundary. If adsorption and desorption at the outer surface of the zeolite crystallites is fast compared to the diffusion inside the pores of the zeolite, adsorption equilibrium can be assumed at the crystal

boundary. This seems a reasonable approach as the diffusion inside the micropores is usually quite slow. An advantage of this approach is that the parameters describing adsorption–desorption at the boundary can be replaced by a single equilibrium adsorption constant, K_a. This takes care of the problem that two parameters need to be fitted which are not completely independent, as was already reported by Nijhuis et al.[19] To check whether adsorption equilibrium can be safely assumed, results for the model described previously can be compared with those from a model assuming adsorption equilibrium.

On the assumption that adsorption–desorption is fast compared to diffusion in the zeolite micropores, the mass flux through the boundary of the zeolite is determined by diffusion to the boundary of the crystal. Equation 4 then has to be replaced by

$$N_c = -D_c \frac{\partial C_x}{\partial x}\bigg|_{x=R_c} \tag{11}$$

The boundary equation at the crystal surface, eq 7, can be replaced by a simple equilibrium condition

$$C_x(x=R_c,z,t) = K_a C_z(z,t) \tag{12}$$

An estimate of the rate of adsorption can be obtained from kinetic gas theory.[24] The number of collisions between molecules and the surface can be calculated using the following relation:

$$\Phi_s = \frac{1}{4} C_{gas} \sqrt{\frac{R_g T}{2\pi M}} \tag{13}$$

which gives the collision rate per unit surface (in moles per square meter) with C_{gas} being the concentration of the gas phase, R_g being the gas constant, T being the temperature, and M being the molar mass of the molecules. The rate constant for adsorption can be calculated from this by dividing this expression by the gas phase concentration. It should, however, be realized that the value calculated from eq 13 gives an upper bound for the true adsorption rate, as not all collisions with the zeolite crystal surface will result in the adsorption of a molecule inside the micropores (i.e., there exists a "surface barrier" for adsorption and the sticking coefficient is smaller than 1). Estimation of the sticking coefficient is not straightforward, and it might have values ranging from approximately 1 to 10^{-3}.

To determine in which regime the models give similar results, a number of simulations have been performed. For the bed porosity, crystal radius, flow rate, and temperature, identical parameters were chosen as those used in the experiments. For the diffusion constant, D_c, a value of 5×10^{-11} m^2 s^{-1} was chosen, which is the upper limit of this parameter found experimentally. The adsorption equilibrium constants found for these systems are typically in the range of 300–1000, so a value of 500 was chosen. This value was, furthermore, used to fix the ratio between the adsorption and desorption constant, as both models should yield equivalent loadings at equilibrium. The upper limit for the rate of adsorption was calculated using eq 13 and was found to be on the order of 80 m s^{-1}. For $K_a = 500$, this corresponds to a desorption rate equal to $k_d = k_a/K_a = 0.16$ m s^{-1}.

Figure 2 shows the simulated concentration profiles at different detector positions along the axis of the reactor (7, 13.1, and 19.2 mm) using the equilibrium model and using the first-order adsorption–desorption model for different values of k_a.
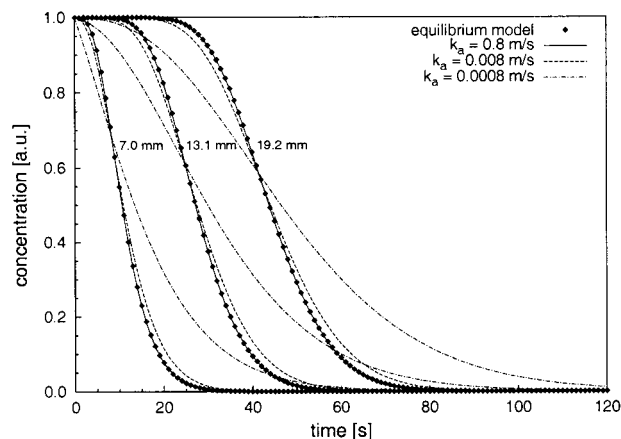

Figure 2. Simulated concentration profiles at $z = 7$, 13.1, and 19.2 mm along the reactor axis for the model assuming adsorption equilibrium (dots) and for different values for the adsorption rate using the model explicitly accounting for adsorption–desorption at the crystal boundaries (lines). Deviations from the equilibrium model only start to be visible for adsorption rates smaller than 0.01 m s^{-1}.

For a value of $k_a = 0.8$ m s^{-1}, the equilibrium model is in perfect agreement with the full model. Only for values smaller than 8×10^{-3} m s^{-1}, meaning that only 1 in 10^4 collisions will lead to adsorption, small deviations between the two models can be observed. For lower values of k_a, the reexchange process is increasingly determined by the rate of desorption at the crystal boundary. Although exact values for the adsorption and desorption rate cannot be obtained, it seems unlikely that the sticking coefficient for the adsorption process on the zeolite crystal surface is smaller than 10^{-4}, and the use of the equilibrium model (thereby neglecting the existence of transport resistances due to a "surface barrier") is justified under the conditions used in this study.

From these results, a criterion can be derived for the importance of adsorption–desorption at the crystal boundary by making use of a modified Biot number for mass transport, Bi_m. Usually, Bi_m is defined as the ratio of the time constants for external film to internal mass transfer resistance (e.g., see Emig and Dittmeyer[25]), but in this case, it can be defined as the ratio between desorption and micropore diffusion

$$Bi_m = \frac{k_d R_c}{D_c} \tag{14}$$

Apparently, the intracrystalline diffusion is slow compared to desorption if the Biot number is greater than 10.

D. Influence of the Diffusion and Adsorption Constants. To be able to extract reliable data from the experiments, the different parameters of interest must have a significant influence on the shape of the exchange curves. Figure 3 shows that under the conditions used in this study, this is indeed the case. For the values of the different model parameters, typical values were chosen as found during the experiments. In a previous study, it was already shown that the influence of axial diffusion can be neglected in this system.[14] Figure 3a shows the effect of varying the adsorption constant while having a fixed value for the micropore diffusion constant. Clearly, variation of this parameter has a large influence on the observed reexchange curves at different positions along the reactor. The same holds for the diffusion coefficient when keeping the adsorption constant fixed, as shown in Figure 3b. Furthermore, it can be concluded that both parameters have a different influence on the measured exchange curves. The adsorption constant mainly determines
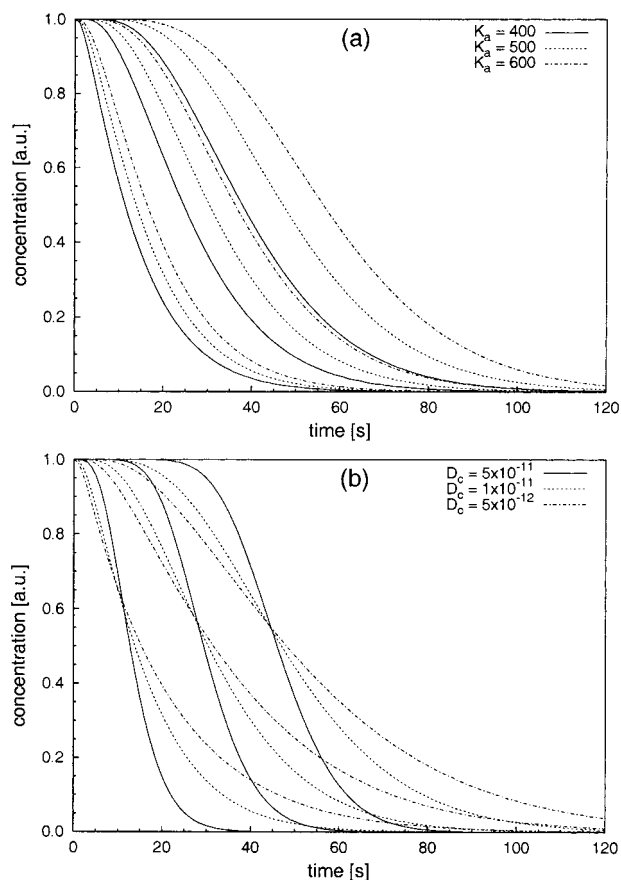
Figure 3. Modeled tracer-reexchange curves at three different positions along the reactor axis (7, 13.1, and 19.2 mm) for (a) different values of the adsorption constant K_a using a fixed value of $D_c = 1 \times 10^{-11}$ m^2 s^{-1} and (b) different values of D_c using a fixed value of $K_a = 500$.

the time scale at which the change in concentration travels through the bed without influencing the actual shape of the curves. The diffusion constant, however, mainly influences the shape of the curves and causes an increasing amount of tailing with decreasing diffusivity. Clearly, analysis of the shape of the tracer-reexchange curves will yield information on both the diffusion constant and the adsorption constant of the molecules under study.

IV. Results and Discussion

The model described above has been used for studying the adsorptive and diffusive behavior of a mixture of *n*-hexane and 2-methylpentane as a function of the mixture composition. The total hydrocarbon pressure was fixed at 6.6 kPa, and the experiments were conducted at a temperature of 433 K. At different mixture ratios, the tracer reexchange of both *n*-hexane and 2-methylpentane was recorded. Figure 4 shows examples of the tracer-reexchange curves at different positions along the reactor for *n*-hexane and 2-methylpentane in a 1:1 mixture. As can be seen, the model accurately describes the measured concentration profiles. The somewhat larger amount of scattering in the experimental 2-methylpentane curves results from a slightly lower yield of this component during the production of labeled hydrocarbons. The plots, furthermore, show that the transport properties of *n*-hexane and 2-methylpentane in this mixture are different. The reexchange of the branched molecule is slower than that of the linear component, indicating that micropore diffusion is faster in the latter case. The larger separation in time of the exchange curves for the linear alkane indicates that this component has a larger adsorption constant.
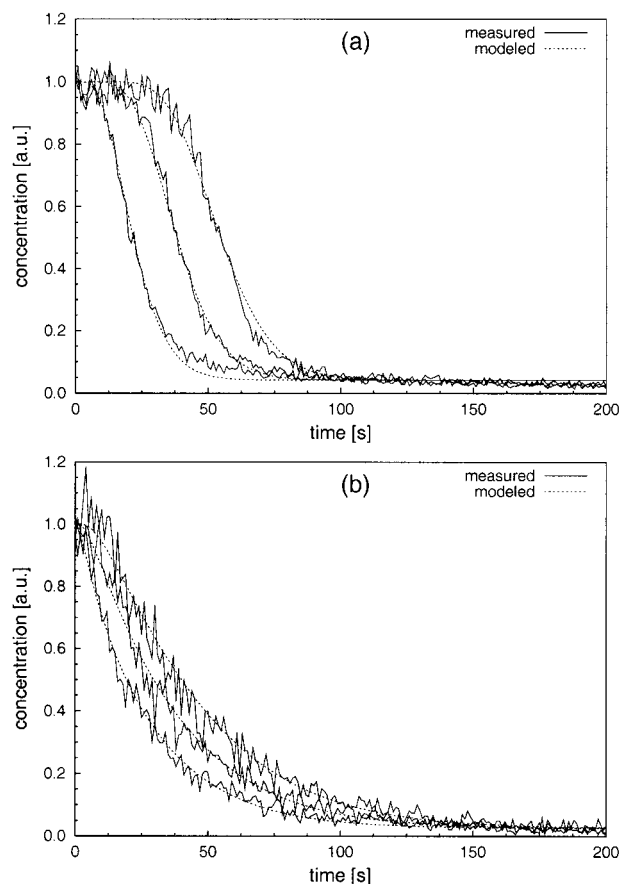

Figure 4. Experimental and simulated tracer-exchange curves at different positions along the reactor axis for (a) *n*-hexane and (b) 2-methylpentane in a 1:1 *n*-hexane/2-methylpentane mixture at 433 K and 6.6 kPa total hydrocarbon pressure.

TABLE 1: Single-Component Loadings at a Temperature of 433 K and a Pressure of 6.6 kPa

adsorbent	loading [mmol/g]	loading [molecules per unit cell]
n-hexane	0.63	3.6
2-methylpentane	0.59	3.4

A. Adsorption of Single Components: Comparison with Literature Data. Although the amount of data on the adsorption and diffusion of mixtures is really limited, there is a fair amount of data on single-component adsorption of *n*-hexane and also some data on that of 2-methylpentane. The adsorptive and diffusive properties of both components have been measured using the TEX-PEP technique. From the fitted adsorption equilibrium constants, the loading (in moles per gram of zeolite) can be calculated using the following relation:

$$\theta = \frac{K_a p_{hc}}{\rho_z R_g T} \tag{15}$$

in which p_{hc} is the hydrocarbon partial pressure, ρ_z is the density of the zeolite, R_g is the gas constant, and T is the temperature. The calculated loadings for *n*-hexane and 2-methylpentane are shown in Table 1. For *n*-hexane, this is in good agreement with the value obtained by Yang and Rees[26] (3.9 molecules per unit cell) and Van Well et al.[27] (3.7 molecules per unit cell). The slightly lower value obtained in this study might be attributed to the higher temperature used (433 instead of 423 K). For 2-methylpentane, extrapolating the data obtained by Cavalcante
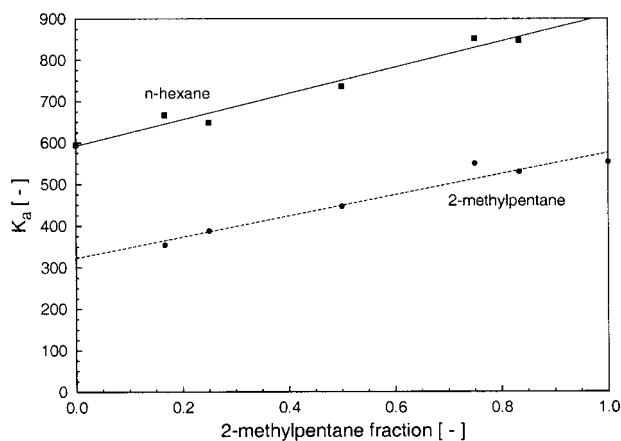
Figure 5. Fitted adsorption constants for *n*-hexane and 2-methylpentane as a function of the 2-methylpentane fraction in the gas phase of the binary mixture.

Figure 6. *n*-Hexane and 2-methylpentane loading as a function of the 2-methylpentane fraction in the gas phase in a binary mixture. The solid symbols are measured loadings; the open symbols are loadings as calculated from configurational-bias Monte Carlo simulations.

and Ruthven[28] to the conditions used in this study yields a value of 2.6 molecules per unit cell, somewhat lower than the value found here. The slightly reduced loading of the branched compared to the linear alkane under equal conditions is in accordance with other studies (e.g., see Vlugt et al.[29]). This is an entropic effect as the adsorption enthalpies of both components are approximately equal but the conformations of the bulkier branched alkanes are much more restricted in the narrow pores of the zeolite. Adsorption of 2-methylpentane from the gas phase thus leads to a higher reduction in entropy compared to adsorption of *n*-hexane, making it entropically less favorable to adsorb the branched isomer.[29]

A comparison between single-component diffusivities obtained with this technique and values from literature has been discussed previously,[14] showing that a reasonable agreement was obtained with previously reported values using other techniques.

B. Binary Adsorption: Results and Comparison with CBMC Simulations. Figure 5 shows the fitted adsorption constants (K_a) for both *n*-hexane and 2-methylpentane as a function of the mixture composition. The error margins in the calculated adsorption constants are around 10%. As can be seen from this plot, the equilibrium adsorption constant for both components increases with increasing 2-methylpentane fraction in the gas phase. This might be due to the slightly lower loading of the branched alkane in single-component systems, as can also be seen from the slightly lower adsorption constant for pure 2-methylpentane compared to that for *n*-hexane. The larger increase of the adsorption constant for *n*-hexane furthermore shows that competitive adsorption of both components is present. This can be seen more easily by plotting the loadings calculated from these adsorption constants.

The solid symbols in Figure 6 show the loadings of both *n*-hexane and 2-methylpentane, as well as the total loading, as a function of the gas phase mixture composition. Obviously, the *n*-hexane loading monotonically decreases and the 2-methylpentane loading monotonically increases with an increasing partial pressure of the branched alkane. The total hydrocarbon loading varies only little (apart from experimental errors) and shows a slight decrease at high 2-methylpentane ratio, as was explained in the previous paragraph. The small deviations from a linear dependence on the mixture composition ratio indicate a small preferential adsorption for *n*-hexane compared to its monobranched isomer. Although the preference for the adsorption of *n*-hexane is small, it does not entirely fall in the inaccuracy of the values determined and was confirmed by repeated experiments.
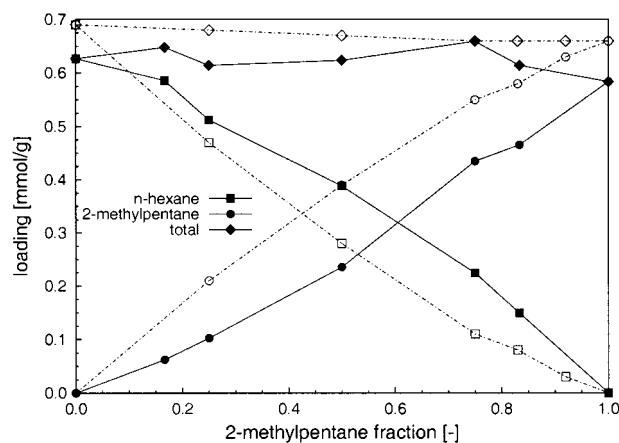
In the literature, different types of adsorptive behavior of binary mixtures have been reported. Cottier et al.,[30] for example, found that for the adsorption of a mixture of *para-* and *ortho*-xylene in various Y-type zeolites, both components essentially behaved similarly to the single-component case and adsorbed independently. A completely different behavior was observed for ethane and ethylene in zeolite 13X by Buffham et al.,[31] where the ethylene was preferentially observed at low ethane partial pressures and a nonlinear dependence thus was observed. A similar behavior was observed by Heuchel et al.[3] for CF_4 and CH_4 in silicalite. The system under study appears to have an identical behavior as the last two systems.

The adsorptive behavior found in this study is in line with a recent configurational-bias Monte Carlo study on the adsorptive behavior of linear and branched alkanes and their mixtures by Vlugt et al.[29] Although their results cannot be directly related because the simulations were performed with a fixed mixture ratio at a lower temperature (300 K), further insight can be gained from this study. From their simulations, they concluded that at a total loading of approximately 4 molecules per unit cell, the loading of the branched alkanes reaches a maximum value. At lower loadings, both components adsorb independently, while at higher loadings the branched alkanes will be squeezed out by the linear alkanes. The peculiar behavior shown by this mixture could be explained when looking at the siting of both components. Vlugt et al. found that while the *n*-hexane could be adsorbed anywhere in the silicalite pores, 2-methylpentane was located at the intersections between the straight and zigzag channels. As a result of that, *n*-hexane has a higher packing efficiency and it is thus easier (or entropically more favorable) to obtain higher loadings with the linear instead of the branched alkanes. For the CH_4/CF_4 system, different sitings for both components were also observed.[32]

Apparently, under the conditions used in the present study, the system is in the regime at which the 2-methylpentane is starting to be pushed out. As a result of the higher packing efficiency of *n*-hexane, as explained above, there is a preference for adsorbing this component. The linear alkane is being replaced only at higher 2-methylpentane fractions, and a nonlinear dependence on the mixture ratio is observed.

To be able to better compare the results obtained from configurational-bias Monte Carlo (CBMC) simulations with the present study, a number of simulations have been performed under equal conditions as used in this work. The calculated loadings from these simulations are shown as open symbols in
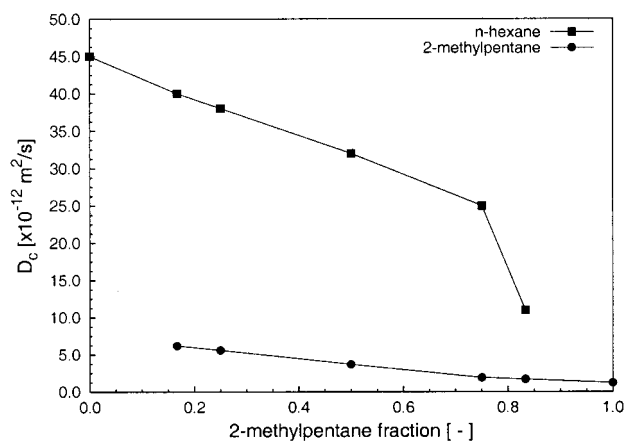
Figure 7. Self-diffusion constant as a function of 2-methylpentane fraction in the gas phase for *n*-hexane and 2-methylpentane at 433 K and a hydrocarbon pressure of 6.6 kPa.

Figure 6. Details about the CBMC simulation technique and the zeolite and alkane models used can be found in Smit and Siepmann[33] and Vlugt et al.[29] The calculated loadings of the single components are slightly higher than the values obtained from TEX-PEP measurements. This is probably due to the use of a perfect crystal structure in the simulations and the pressence of defects in the silicalite crystals used in this study. The slight decrease of the total loading is predicted correctly by the simulations. The slight preference for the adsorption of *n*-hexane, however, is not observed, but instead, a (very) small preference for the branched alkane is seen. This can probably be attributed to imperfections in the model parameters used for the CBMC simulations.

C. Multicomponent Diffusion. Figure 7 shows the diffusion coefficients as obtained from the TEX-PEP experiments for *n*-hexane and 2-methylpentane as a function of the gas phase composition. Obviously, the diffusivity of pure *n*-hexane is much higher than that of the larger 2-methylpentane molecules (approximately a factor of 9). For both components, a decrease in mobility is observed with an increasing fraction of the branched alkane in the gas phase. The 2-methylpentane behaves essentially in a way one would expect for a single-component system (e.g., see Schumacher and Karge[34] and Schuring et al.[35]), whereby the diffusivity monotonically decreases with increasing loading of this component. The diffusivity of the faster *n*-hexane depends more strongly on the composition of the gas mixture. Because the loading of *n*-hexane decreases with increasing 2-methylpentane fraction but the total loading remains approximately constant, this decrease in mobility must result from interactions with its branched isomer in the system. Most remarkable is the sudden drop in diffusivity above a 2-methylpentane fraction of 0.75.

The diffusivity of molecules inside the zeolite lattice depends strongly on the loading of the zeolite crystal.[35] The plot shown in Figure 7 should therefore be treated with some caution, as the dependency of the diffusion constant on the gas phase composition is also influenced by the adsorptive behavior of the alkanes. In this case, however, the influence of adsorption is limited because the total loading remains constant and there is only a small preferential adsorption for *n*-hexane. The results can therefore be directly related to MD studies from other authors, where one commonly uses a fixed total loading and diffusivities as a function of the adsorbed phase fraction.

For 2-methylpentane fractions lower than 0.75, the behavior found in this study is essentially identical to that obtained in other studies.[4,10,36] In all these systems, it was found that the

diffusivity of the slow component is essentially unaffected by the presence of the fast component. The diffusive behavior can be understood on the basis of a simple jump diffusion model, in which diffusion is thought of as a sequence of activated jumps from one site to another, as was already demonstrated by Masuda et al.[10] Such a jump can only be successful if the site to which the molecule jumps is empty. Although the jump frequency itself does not depend on the composition of the mixture, the number of successful jumps will. When the amount of slowly moving molecules (2-methylpentane) increases, they will essentially block the channel segments and the number of successful jumps of the fast component (*n*-hexane) will be determined by the rate at which an empty site is created by a jump of the slow component. At high 2-methylpentane loadings, the diffusivity of *n*-hexane will thus be strongly determined by the diffusion rate of its branched isomer. The dependency of the 2-methylpentane diffusivity itself on mixture composition observed in this study is mainly caused by the relatively high total loading at the conditions used. In this case, the interactions between the branched alkanes themselves play an important role and will seriously decrease the mobility of the slow-moving component at higher fractions in the gas phase. This was also observed in the work by Jost et al.,[4] where the slow component (in this case xenon) showed an increasing dependency on the mixture composition with increasing total loading of the zeolite.

The sudden drop in the diffusivity of *n*-hexane at a ratio above 0.75 is due to the particular adsorptive properties of both components in silicalite. As was shown by Vlugt et al.,[29] 2-methylpentane preferentially adsorbs in the intersections between straight and zigzag channels. When all the intersections are occupied by the slowly diffusing branched alkanes, the entire pore system will essentially be blocked and diffusion of the fast component will be totally determined by the hopping rate of the slow component moving from one intersection to another. This is strongly supported by the fact that the sudden drop in diffusivity takes place at a 2-methylpentane loading of about 3 molecules per unit cell, as each unit cell of silicalite contains three channel intersections. A similar effect was observed in a system of methane and benzene in zeolite NaY[37] and silicalite.[38] In NaY, the benzene molecules effectively block the windows of the supercages for the faster methane. Förste et al.[38] showed that the decrease of methane diffusivity was also caused by blocking of the channel intersections by benzene in zeolite silicalite.

The results obtained here emphasize the importance of the structure of the zeolite channels when looking at multicomponent diffusion. The sudden drop in diffusivity of the fast component in this system is a direct result of the adsorptive behavior of both components and the channel topology of the zeolite. This explains why a similar behavior was not observed in previous studies. For example, for the methane/xenon[4] and methane/tetrafluoromethane[32] mixtures in silicalite, both components are preferentially sited in the interiors of the (straight and zigzag) channels, causing the blocking by the slow components to be less dramatic. For the *n*-butane/methane system,[36] the fast component (methane) shows a slight preference for adsorption in the intersections, while the slow component resides in the channels. Although the results cannot be directly compared, an accelerated drop was indeed observed but only at much higher loadings.

The dependency of multicomponent diffusion on adsorption properties and zeolite topology has some important consequences for the description of mass transfer in binary systems. Usually, the transport of these mixtures in a packed zeolite bed

during transient experiments will be described by diffusion equations, using diffusion constants which are independent of the loading. The current results show that this is definitely not the case, as the diffusivity can be a strong function of the mixture composition. A more advanced approach for describing mass transfer is provided by the Maxwell−Stefan theory, which has been applied successfully to diffusion and adsorption in zeolites.[39,40] In a recent study, Krishna showed that this theory could indeed describe the behavior as observed in MD simulations of methane/xenon, methane/CF$_4$, and methane/*n*-butane.[40] However, although the Maxwell−Stefan theory accounts for sorbate−sorbate interactions, it does not explicitly incorporate the pore structure and siting of the molecules and will thus fail to describe the phenomena shown in this work. Whether the multicomponent diffusivity can be predicted from single-component diffusivities will thus depend on the particular system under study, and a general application of the Maxwell−Stefan theory should be treated with caution. Instead, more detailed model descriptions are needed to gain insight into the diffusive behavior. Among these descriptions are Monte Carlo lattice dynamics simulations[41,42] and percolation theory.[43]

Also for systems in which reactions take place, the behavior observed here might have some important implications. The *n*-hexane/2-methylpentane mixture could represent a reactant/product system. In that case, the mobility can become a strong function of the radial coordinate of the crystal. In extreme cases, reactants or products could be piled up inside the crystals, essentially blocked by the slow components present in the system, thus, having a serious effect on the activity of the catalyst.

V. Conclusions

In this work, the tracer-exchange positron emission profiling (TEX-PEP) technique has been used for determining the adsorptive and diffusive properties of an *n*-hexane/2-methylpentane mixture at elevated temperatures (433 K). With this technique, the reexchange of radioactively labeled molecules can be studied as a function of time and position inside the reactor. Because only one of the components in the feed is labeled, the mass transport properties of each individual component can be determined. Determination of these properties is done by fitting a numerical model for mass transfer in a packed zeolite bed to the measured concentration profiles accounting for convection, adsorption at the crystal boundary, and diffusion between and inside the crystals. Under the conditions used in this study, the adsorption−desorption process at the crystal boundary does not have to be explicitly accounted for because the diffusive process is the rate-determining process at the crystal surface.

The system shows a slight preference for the adsorption of *n*-hexane over 2-methylpentane. This is due to the fact that it is entropically more favorable to adsorb the linear alkane because it can reside anywhere in the pore system, while the branched alkane is preferentially adsorbed in the intersection between straight and zigzag channels. This is in line with the conclusions obtained from the CBMC simulations of Vlugt et al. (1999) at lower temperatures and a constant mixture ratio. CBMC simulations performed at similar conditions as in this work show a reasonable agreement, although a slightly different behavior is predicted by these calculations.

As was also observed in earlier studies, the diffusion of the fast-moving *n*-hexane molecules is strongly influenced by the presence of the slowly diffusing 2-methylpentane. The measure-

ments, however, show a large drop in diffusivity at a large 2-methylpentane fraction in the gas phase. Most likely, this is due to the blocking of the channel intersections by the slowly moving branched alkanes, as this sudden drop takes place at a 2-methylpentane loading of approximately 3 molecules per unit cell, equal to the number of intersections in this cell. This indicates that the adsorptive properties of the different components, together with the topology of the zeolite pores, play an important role in the behavior of multicomponent systems. Models based on mean field approximations of the diffusion, like Fick's law and Maxwell−Stefan diffusion, should therefore be treated with caution.

References and Notes

(1) Kärger, J.; Ruthven, D. M. *Diffusion in zeolites and other microporous solids*; Wiley−Interscience: New York, 1992.

(2) Kärger, J. In *Handbook of Catalysis*; Ertl, G., Knözinger, H., Weitkamp, J., Eds.; VCH: Weinheim, Germany, 1996; Vol. 3, pp 1252−1261.

(3) Heuchel, M.; Snurr, R. Q.; Buss, E. F. *Langmuir* **1997**, *13*, 6795.

(4) Jost, S.; Bär, N.-K.; Fritzsche, S.; Haberlandt, R.; Kärger, J. *J. Phys. Chem. B* **1998**, *102*, 6375.

(5) Gladden, L. F.; Sousa-Goncalves, J. A.; Alexander, P. *J. Phys. Chem. B* **1997**, *101*, 10121.

(6) Gergidis, L. N.; Theodorou, D. N.; Jobic, H. *J. Phys. Chem. B* **2000**, *104*, 5541.

(7) Choudhary, N. V.; Jasra, R. V.; Bhat, S. G. T.; Prasada Rao, T. S. R. Studies in Surface Science and Catalysis. In *Zeolites: Facts, Figures, Future,* Proceedings of the 8th International Zeolite Conference, Amsterdam, The Netherlands, July 10−14, 1989; Jacobs, P. A., van Santen, R. A., Eds.; Elsevier: Amsterdam, The Netherlands, 1994; Vol. 49, pp 867−876.

(8) Niessen, W.; Karge, H. G. *Microporous Mater.* **1993**, *1*, 1.

(9) Funke, H. H.; Argo, A. M.; Falconer, J. L.; Noble, R. D. *Ind. Eng. Chem. Res.* **1997**, *36*, 137.

(10) Masuda, T.; Fujikata, Y.; Ikeda, H.; Hashimoto, K. *Microporous Mesoporous Mater.* **2000**, *38*, 323.

(11) Anderson, B. G.; Van Santen, R. A.; Van IJzendoorn, L. J. *Appl. Catal. A* **1997**, *160*, 125.

(12) Anderson, B. G.; Van Santen, R. A.; De Jong, A. M. *Top. Catal.* **1999**, *8*, 125.

(13) Anderson, B. G.; De Gauw, F. J.; Noordhoek, N. J.; Van IJzendoorn, L. J.; Van Santen, R. A.; De Voigt, M. J. A. *Ind. Eng. Chem. Res.* **1998**, *37*, 815.

(14) Schumacher, R. R.; Anderson, B. G.; Noordhoek, N. J.; De Gauw, F. J. M. M.; De Jong, A. M.; De Voigt, M. J. A.; Van Santen, R. A. *Microporous Mesoporous Mater.* **2000**, *35−36*, 315.

(15) Smit, B.; Maesen, L. M. *Nature* **1995**, *374*, 42.

(16) Cunningham, R. H.; Mangnus, A. V. G.; Van Grondelle, J.; Van Santen, R. A. *J. Mol. Catal. A: Chem.* **1996**, *107*, 153.

(17) Mangnus, A. V. G.; Van IJzendoorn, L. J.; De Goeij, J. J. M.; Cunningham, R. H.; Van Santen, R. A.; De Voigt, M. J. A. *Nucl. Instrum. Methods Phys. Res., Sect. B* **1995**, *99*, 649.

(18) Rosen, J. B. *J. Chem. Phys.* **1952**, *20*, 387.

(19) Nijhuis, T. A.; Van den Broeke, L. J. P.; Linders, M. J. G.; Van de Graaf, J. M.; Kapteijn, F.; Makkee, M.; Moulijn, J. A. *Chem. Eng. Sci.* **1999**, *54*, 4423.

(20) Noordhoek, N. J.; Van IJzendoorn, L. J.; Anderson, B. G.; De Gauw, F. J.; Van Santen, R. A.; De Voigt, M. J. *Ind. Eng. Chem. Res.* **1998**, *37*, 825.

(21) Hong, U.; Kärger, J.; Kramer, R.; Pfeifer, H.; Seiffert, G.; Müller, U.; Unger, K. K.; Lück, H.-B.; Ito, T. *Zeolites* **1991**, *11*, 816.

(22) Schiesser, W. E. *The numerical method of lines: integration of partial differential equations*; Academic Press: San Diego, 1991.

(23) Marquardt, D. *SIAM J. Appl. Math.* **1963**, *11*, 431.

(24) Atkins, P. W. *Physical Chemistry*, 3rd ed.; Oxford University Press: Oxford, U.K., 1969; Chapter 25.

(25) Emig, G.; Dittmeyer, R. In *Handbook of heterogeneous catalysis*; Ertl, G., Knözinger, H., Weitkamp, J., Eds.; VCH: Weinheim, Germany, 1996; Vol. 3, pp 1209−1252.

(26) Yang, Y.; Rees, L. V. C. *Microporous Mater.* **1997**, *12*, 117.

(27) Van Well, W. J. M.; Wolthuizen, J. P.; Smit, B.; Van Hooff, J. H. C.; Van Santen, R. A. *Angew. Chem., Int. Ed. Engl.* **1995**, *34*, 2543.

(28) Cavalcante, C. L.; Ruthven, D. M. *Ind. Eng. Chem. Res.* **1995**, *34*, 177.

(29) Vlugt, T. J. H.; Krishna, R.; Smit, B. *J. Phys. Chem. B* **1999**, *103*, 1102.

(30) Cottier, V.; Bellat, J.-P.; Simonot-Grange, M.-H.; Méthivier, A. *J. Phys. Chem. B* **1997**, *101*, 4798.

(31) Buffham, B. A.; Mason, G.; Heslop, M. J. *Ind. Eng. Chem. Res.* **1999**, *38*, 1114.

(32) Snurr, R. Q.; Kärger, J. *J. Phys. Chem. B* **1997**, *101*, 6469.

(33) Smit, B.; Siepmann, J. I. *J. Phys. Chem.* **1994**, *98*, 8442.

(34) Schumacher, R. R.; Karge, H. G. *J. Phys. Chem. B* **1999**, *103*, 1477.

(35) Schuring, D.; Jansen, A. P. J.; Van Santen, R. A. *J. Phys. Chem. B* **2000**, *104*, 941.

(36) Gergidis, L. N.; Theodorou, D. N. *J. Phys. Chem. B* **1999**, *103*, 3380.

(37) Nivarthi, S. S.; Davis, H. T.; McCormick, A. V. *Chem. Eng. Sci.* **1995**, *50*, 3217.

(38) Förste, C.; Germanus, A.; Kärger, J.; Pfeifer, H.; Caro, J.; Pilz, W.; Zikánová, A. *J. Chem. Soc., Faraday Trans. 1* **1987**, *83*, 2301.

(39) Kapteijn, F.; Moulijn, J. A.; Krishna, R. *Chem. Eng. Sci.* **2000**, *55*, 2923.

(40) Krishna, R. *Chem. Phys. Lett.* **2000**, *326*, 477.

(41) Paschek, D.; Krishna, R. *Phys. Chem. Chem. Phys.* **1999**, *2*, 2389.

(42) Coppens, M.-O.; Bell, A. T.; Chakraborty, A. K. *Chem. Eng. Sci.* **1998**, *53*, 2053.

(43) Keffer, D.; McCormick, A. V.; Davis, H. T. *J. Phys. Chem.* **1996**, *100*, 967.